Soft Matter

The Influence of Additives on Polymer Matrix Mobility and the Glass Transition

Journal:	*Soft Matter*
Manuscript ID	SM-ART-09-2020-001634.R1
Article Type:	Paper
Date Submitted by the Author:	19-Oct-2020
Complete List of Authors:	DeFelice, Jeffrey; Dartmouth College, Chemistry Lipson, Jane; Dartmouth College, Chemistry

The Influence of Additives on Polymer Matrix Mobility and the Glass Transition

Jeffrey DeFelice
Department of Chemistry,
Dartmouth College, Hanover, NH 03755
Jane E. G. Lipson*
Department of Chemistry,
Dartmouth College, Hanover, NH 03755

Abstract

In the region near an interface, the microscopic properties of a glass forming liquid may be perturbed from their equilibrium bulk values. In this work, we probe how the interfacial effects of additive particles dispersed in a matrix can influence the local mobility of the material and its glass transition temperature, T_g. Experimental measurements and simulation results indicate that additives, such as nanoparticles, gas molecules, and oligomers, can shift the mobility and T_g of a surrounding polymer matrix (even for relatively small concentrations of additive; e.g., 5-10% by volume) relative to pure bulk matrix, thus leading to T_g enhancement or suppression. Additives thus provide a potential route for modifying the properties of a polymer material without significantly changing its chemical composition. Here we apply the Limited Mobility (LM) model to simulate a matrix containing additive species. We show that both additive concentration, as well as the strength of its very local influence on the surrounding matrix material, will determine whether the T_g of the system is raised or lowered, relative to pure matrix. We demonstrate that incorporation of additives into the simple LM simulation method, which has successfully described the behavior of bulk and thin film glassy solids, leads to direct connections with available experimental and simulation results for a broad range of polymer/additive systems.

Introduction

Additives such as small organic molecules,[1-3] gases,[4-13] ionomers,[14] and nanoparticles[15-24] can influence the properties of the surrounding polymer matrix relative to those of the pure bulk. Some examples of the physical properties that can be shifted by the presence of additives are mechanical properties,[3,7,25-27] membrane permeability,[8-11,19,28-37] and the glass transition temperature, T_g [3,11,15-20,31,34,38-40]. In this work, we apply a simple kinetic lattice simulation approach, the Limited Mobility (LM) model[41-45], to probe the ways in which non-reactive additives distributed throughout a sample can influence the local mobility of a polymer melt, and therefore the sample T_g , relative to that of the pure bulk fluid. Using the LM model we can control the extent to which additives perturb their local environment, allowing comparisons with a number of chemically distinct bulk polymer/additive systems.

Additives are commonly regarded as mobility enhancing (plasticizing) or mobility reducing (antiplasticizing). Those that enhance matrix mobility lower the activation energy barrier for segmental relaxations of the surrounding polymer molecules to occur. Experimental measurements[25,30-33,35,46-50] and simulations[3,11,15-18,26,34,38-40,51-53] have shown that plasticizing additives reduce the segmental relaxation time, τ, in comparison to that of the pure bulk. Some of these studies have attributed the reduction in τ caused by the addition of plasticizing particles to an enhancement in matrix free volume[6,36,37,51,52,54]. For example, plasticizing additives can frustrate the local segmental packing, thus favoring chain conformations that lead to an increase in the free volume, and therefore local density, or mobility, of the surrounding matrix. Accompanying the change in τ and local mobility concomitant changes in other important material properties can also occur. One notable example for which plasticization impacts material functionality is in the case of gas separation membranes[8-11,19,28-37]. As gas molecules enter the membrane from the upstream side, the concentration of gas molecules inside the membrane grows, which enhances the membrane permeability. However, due to the membrane permeability-selectivity "trade-off",[36] the sorption of gas molecules which increases membrane permeability, comes at the expense of its selectivity to separate one gas species from another. This is a particularly common limitation for CO_2 separation polymer membranes, because CO_2 has a strong plasticizing effect on a number of polymer species[25,30-33,35,46-49].

As noted above, the role of anti/plasticizers can be linked to changes in material mobility and thus, to modulus. A number of experimental measurements indicate that plasticizing additives can reduce the matrix T_g relative to that of the pure bulk[25,30,32,33,35,46-49,51]. The extent of this T_g reduction increases as the concentration of plasticizer increases. For example, differential scanning calorimetry (DSC) measurements performed on a variety of polymer species showed that a ~50% reduction in T_g occurs in the presence of ~5 MPa of CO_2. [28] Molecular Dynamics (MD)[3,11,15-18,26,38-40,51,52] and Monte Carlo (MC) simulations[19,20,34,55] have also been applied to polymer/plasticizer systems, the results of which were consistent with the experimental measurements; i.e., plasticizers lower the T_g of the matrix via a reduction in the relaxation time of the molecules in the surrounding matrix.

Turning to antiplasticizing additives, these particles generally reduce mobility in the surrounding matrix, i.e., increase the relaxation time of the surrounding molecules, relative to that of the pure bulk. However, as noted by Mangalara and Simmons[3] and supported by experimental evidence,[26,40,56] simply characterizing an additive as "antiplasticizing" does not adequately encompass the range of possible changes that may occur to the physical properties of the matrix. For example, the antiplasticization effect on matrix mobility may exhibit a temperature dependence; i.e., an antiplasticizer may *reduce* matrix mobility at high temperatures, while *enhancing* mobility relative to that of the pure bulk at low temperatures, *or* vice versa[26]. When the low temperature mobility is enhanced (reduced) by an antiplasticizer, the T_g of the matrix is lowered (increased) relative to that of the pure bulk value[3,15,26,40,56]. In work by Kalogeras and coworkers,[56] the changes in T_g for poly(methyl methacrylate) (PMMA) doped with a variety of chemically distinct luminescent organic dye molecules were studied. They observed both T_g enhancement and T_g suppression of PMMA, depending on the chemical nature of the organic dye[56]. Using a bead-spring model, Mangalara and Simmons[3] simulated a range of flexible to stiff oligomeric additives in a polymer melt, from which they concluded that it is possible for additives to enhance the glassy modulus (G_∞) while simultaneously increasing *or* decreasing τ and T_g.

The T_g changes observed for polymer/additive systems often draw comparisons with the thickness dependent T_g behavior reported for nanometrically thin polymer films[1,2,21,22,38]. One reasonable connection that can be made between polymer/additive and film systems is through the role that interfaces play in influencing their physical properties. In a polymer/additive system, the

polymer-additive "interfaces" are distributed throughout the material, whereas for a polymer film, the interfaces (e.g., a free surface or substrate) occur at the boundaries of the material. In the region of a film near an interface, the local properties may differ from those of the bulk; e.g., segmental relaxation time, molecular packing, and the local T_g[57-71]. As the total film thickness decreases, the relative size of the interfacial region grows with respect to that of the total film thickness[63,66-68,41,72,73]. Experimental measurements[57-59,74-85] and theoretical studies[60-62,69,86-88] have suggested that the perturbations to the local properties caused by an interface can play a substantial role in influencing the global properties of a film, such as its T_g, as the total film thickness decreases. By changing the nature of the polymer film's interface, thickness-dependent T_g enhancement[66-68] and suppression[67,73] have been observed. This is analogous to changing from a plasticizing to an antiplasticizing additive in a polymer matrix. Further, additives can also be included in polymer films themselves, for which it has been reported that the thickness-dependent T_g behavior of pure films can be modified by doping with nanoparticles,[1,2,21,22,38] or in the case of membranes, upon gas sorption[4-13]. Therefore, the characterization of polymer/additive bulk systems can provide useful insight that is applicable to polymer films and membranes.

In this work we apply the Limited Mobility (LM) model for the first time to simulate polymer/additive mixtures. Previous applications of the LM model include: pure bulk, buried slab, and film systems.[41-45] Both for the studies on bulk material and on free-standing and supported films the LM model has proven very successful in capturing experimental trends without optimizing simulation parameters; indeed, in some cases the agreement was better than semi-quantitative. In this work we show that the LM simulation model with additives captures a broad set of experimental trends, reflecting an additive range which spans dissolved gas to silica nanoparticles, to small organics. This very simple simulation approach demonstrates that tuning the effectiveness of an additive in influencing very local matrix mobility translates into an ability to control the direction extent of the shift in the material's glass transition temperature.

This paper is organized as follows: In the next section, we provide a brief overview of the LM model, which includes a description of how additive particles have been introduced. The Results and Discussion section that follows divides the results into different categories: In part 1 we study the influence of additives on matrix mobility. In part 2, we demonstrate that LM additives

can serve as plasticizers and as antiplasticizers, and make connections to other work in the literature. In part 3 we turn to T_g changes with respect to additive concentration, addressing the extent to which T_g can be shifted as a function of additives having a range of characteristic properties. In part 4 we examine how the properties of the matrix itself influence the extent of the additive induced effect on T_g . We conclude this section with part 5, in which T_g trends are examined as the additive nature is more broadly varied for three fixed additive concentrations. The paper ends with our Summary and Conclusions.

The Limited Mobility (LM) Simulation Model

The LM model is a kinetic lattice model, where each lattice site represents a fluid element in two-dimensions. For a pure bulk system, each site corresponds to one of three possible states: "mobile", "dormant", or "dense" [41,43,45]. These states represent three possible designations of relative mobility, as suggested by fluid simulations: mobile, dormant, and dense, respectively[89,90]. A "mobile" site represents a localized "active" region within a fluid, where particles can locally diffuse via "string-like" motion,[90] or locally relax via dispersion of mobility[89]. The latter situation results in a site being considered "dormant". A dormant site can evolve to become mobile; however, it cannot happen independently. A nearest neighbor mobile site is required in order to facilitate the transition of a dormant site to become mobile.

Details of initializing and running the LM model are elaborated upon below. Relatively few parameters need to be specified in this simulation approach: The temperature must be set, along with parameters that characterize the nature of the matrix material and that of the additive. These parameters link to the ability of material in an LM site (whether matrix or additive) to influence mobility in neighboring sites, and are discussed more fully below. As the simulation runs, the sample evolves until it equilibrates in a state that may be above, or below, the glass transition (defined below). The arc of this evolution is characterized by tracking the fraction of material in the mobile state.

In this work, we have expanded on the LM model to include a fourth possible state for a lattice site, corresponding to the presence of an "additive". An additive site represents a region in the fluid that is chemically distinct from its surrounding; e.g., gas molecules, small organic molecules, or inorganic nanoparticles dispersed in a polymer matrix. For a matrix system

containing additive sites, we classify the "matrix" portion as being composed of "mobile", "dormant", and "dense" sites. An additive site is different from one in the matrix because it cannot evolve to become "mobile", "dormant", or "dense"; i.e., the concentration of additive sites is chosen at the start of the simulation and remains fixed. This is keeping with the experimental studies referenced, in which even a bulk sample of the additive (for example, a gas such as CO_2, or silica nanoparticles) would not undergo a state change within the experimental parameters used.

The LM model is initialized by randomly assigning mobile, dormant, dense, and additive sites to positions on a 64x64 square lattice. We consider each lattice site to have eight neighbors: four nearest and four next-nearest. First, the initial fraction of additive sites is chosen, which represents the concentration of the additive in a matrix system. [The pure bulk corresponds to a system where the fraction of additive sites is equal to zero, or equivalently, where the entire system is composed of "mobile", "dormant", and "dense" matrix sites only.] Then the remaining sites (i.e., matrix sites) are randomly assigned to be mobile, dormant, or dense such that the initial fractions of each site type are equal.

The system evolves over Monte Carlo loops during which operations are attempted on randomly selected lattice sites, such that one system sweep corresponds to a number of attempted operations that is equal to the total number of lattice sites. Every simulation runs for 5×10^5 system sweeps, followed by an additional 5×10^5 sweeps over which statistics are collected. For matrix sites the attempt probability of each type of operation is 1/3, regardless of the identity of the randomly selected lattice site. The operations possible for matrix sites are illustrated in Figure 1 and described below.

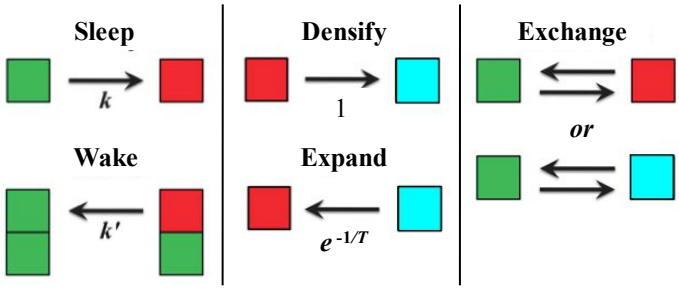

Figure 1: LM moves for "matrix" sites, which consist of green (mobile), red (dormant), and blue (dense) sites.

- *Sleep*/*Wake*: a mobile site may become dormant ("sleep") with probability, *k*. The reverse of this operation, i.e. a dormant site becoming mobile ("wake"), may occur with probability *k'*, and must be *facilitated* by at least one adjacent mobile site.
- *Densify*/*Expand*: a dormant site may become dense ("densify") with probability, 1. The reverse of this operation, a dense site becoming dormant ("expand"), may occur with a probability $e^{-1/T}$. We interpret the inverse temperature analogous to the external field in the Fredrickson-Anderson kinetically constrained Ising model[91].
- *Exchange:* a mobile site may swap positions ("exchange") with a randomly selected neighboring site of any type, i.e. dormant, dense, or mobile, with probability 1. A dormant or dense site may swap with a randomly selected neighbor *only if that neighbor is mobile*, also with a probability of unity.

k and k' characterize the relative tendency of the matrix material in a site to suppress local mobility and to facilitate its propagation. [44] In studies on LM thin films[43] we noted that variation in these parameters controlled mobile layer thickness in a manner analogous to trends found in experimental studies through changing the chemical nature of the material. Experimentally, no simple characteristic material property tracked directly with the trend, however, mobile layer thickness did appear to correlate with enhanced local dynamics. This was mirrored in the LM results through decreasing the ratio k/k'.

We now turn to the new LM model operations that correspond to additive sites, which are given in Figure 2.

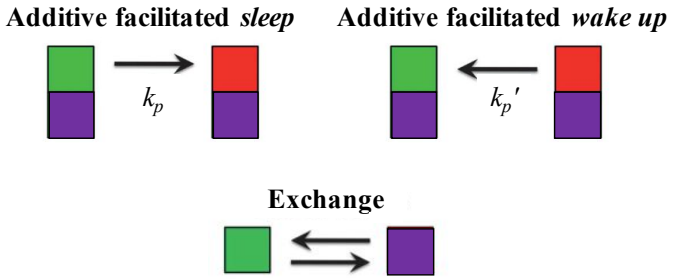

Figure 2: LM moves for additive sites (shown in purple), which represent an additive species (e.g. gas molecules, nanoparticles, etc.).

Randomly selected sites are designated as 'additive' with a probability given by their concentration. In this work, while we investigate effects up to an additive site fraction of 0.30, we are mostly interested in the effects of lower concentrations. Such a site can influence the surrounding matrix via the "additive facilitated sleep and wake up" moves shown in Figure 2. The attempt probability for each (sleep/wakeup or exchange) of 1/2. If the additive site is trying to facilitate a neighboring mobile site to become dormant ("additive facilitated sleep") the probability of success will be equal to k_p; if it is trying to facilitate a neighboring dormant site to become mobile the probability of success will be equal to k_p'. The remaining operation is the "exchange" move, where an additive site can swap positions with a neighboring mobile site with probability 1 (analogous to the "exchange" moves for the matrix sites).

Analogous to the matrix, the k_p and k_p' values characterize the additive ability to facilitate nearby material be more, or less, mobile. For example, dissolved CO_2 might be expected to enhance local mobility, while an additive that could engage in, say, hydrogen bonding with matrix material might be expected to diminish local mobility.

With or without additives, the transition between the melt state and the glassy state is determined by monitoring the average fraction of mobile sites in the matrix material. The expression for $\overline{f}_{\text{matrix}}$ is given by:

$$\overline{f}_{matrix} = \frac{mobile}{mobile + dormant + dense} \quad (1)$$

In prior work[42,44] involving only the *pure bulk* system, it was shown that ratio *k/k'* and *T* control the state of the system and in that case the LM model yields a non-zero (i.e. non-trivial) glass transition temperature, defined to be the temperature at which the fraction of mobile sites falls to zero. Unlike the pure bulk, in systems having one or more *free* surfaces the interface continues to act as an infinite source and sink of mobility in the LM model[41,43,44] , which means that the fraction of mobile sites will not vanish at finite temperature. In contrast to the situation involving a free surface, additive sites in a matrix system will not introduce *new* mobility, however, they will influence mobility via the facilitated interconversion of neighboring mobile and dormant matrix sites; i.e., the additive "sleep" and "wake up" moves. For the present work, in analogy to

the condition applied in prior research using the LM model to simulate films, the glass transition temperature will be identified as that value corresponding to $\overline{f}_{\text{matrix}} = 0.10$,[45] where 0.10 is less than $1/z$, the reciprocal of the number of neighbors (8) per lattice site[92]. In other words, rather than demanding zero mobility as a condition for glassification, we follow a physical picture in which, at the glass transition, a site averages fewer than one mobile neighbor. In order that T_g be consistently determined in both the pure bulk limit and for systems for which interfacial effects (additives) are present we will apply the same criterion in all cases.

Results and Discussion

1. Additive effects on matrix mobility

Recall that the matrix is composed of mobile, dormant, and dense sites only. In Figure 3, we quantify the effect of additive concentration on matrix mobility. We plot the steady state mobile site fraction in the surrounding matrix, $\overline{f}_{\text{matrix}}$, as function of temperature for two initial scenarios: 1) "inert" additive sites and 2) additive sites parameterized to match the matrix. "Inert" additive sites have $k_p = k_p' = 0$, so their only action can be exchanging positions with a neighboring mobile site. This allows us to model a system in which the additive has no effect on local matrix material, and it also serves as a control for illustrating the change from inert to active engagement as k_p and k_p' change. In the second scenario, we parameterize the additive sites such that they match the matrix, i.e. $k = k' = k_p = k_p' = 0.40$. In this case the attempt probabilities of the additive facilitated "sleep" and "wake up" moves match those assigned to the matrix site "sleep" and "wake up" moves.

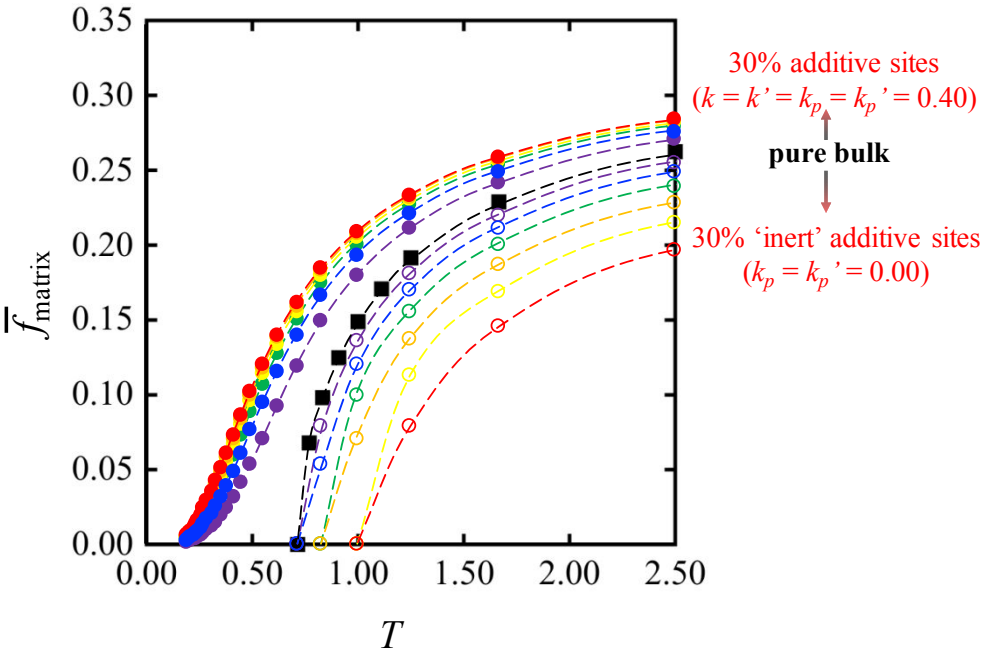

Figure 3: Change in the fraction of mobile site in the matrix, $\overline{f}_{\text{matrix}}$, upon lowering the temperature, T. Results for a pure bulk fluid are shown as black squares, solid points correspond to additive sites with $k = k' = k_p = k_p' = 0.40$ and open points correspond to additive sites with $k_p = k_p' = 0.00$. The colors represent a matrix containing 0.05 (purple), 0.10 (blue), 0.15 (green), 0.20 (orange), 0.25 (yellow), and 0.30 (red) site fraction of additives. Dashed lines are guides to the eye.

In Figure 3 the effect of cooling on matrix mobility is compared as the additive concentration is changed, for two types of additives. The black symbols (and line to guide the eye) show the LM results for a pure bulk matrix material. First consider the effect of inert additive sites ($k_p = k_p' = 0.00$), which is illustrated by the sets of open circles. As the concentration of these sites increases from 0% (pure bulk) to 30%, the steady state fraction of mobile sites in the matrix, $\overline{f}_{\text{matrix}}$, drops more rapidly as the system is cooled. In addition, at any fixed temperature, the fraction of mobile sites in the matrix *decreases* as the concentration of these additive sites *increases*. For example, at $T = 1.00$, $\overline{f}_{\text{matrix}} = 0.15$ in the pure bulk, whereas $\overline{f}_{\text{matrix}} = 0$ for a matrix system containing 30% purple sites. This means that the matrix material containing additives will glassify at a higher temperature than the pure, bulk matrix.

The reduction in mobility observed for a matrix system containing inert additive sites is traceable to the matrix "wake up" move, which requires facilitation by a neighboring mobile site. As the fraction of additive sites increases, the probability that a dormant site has at least one mobile

neighbor is decreased on average, which limits the successful conversion from the dormant to mobile state. This behavior is comparable to the reduction in local mobility observed in the region of a film near a non-interacting substrate in the LM model[41] and suggests an analogous interpretation of our results for the additive induced effect.

Next we turn to additives parameterized to match the matrix ($k = k' = k_p = k_p' = 0.40$). The results shown in Figure 3 (sets of solid points) indicate that for a chosen temperature, the value of $\overline{f}_{\text{matrix}}$ increases relative to that of the pure bulk as the fraction of additive sites increases from 0% to 30%. As the temperature is lowered, $\overline{f}_{\text{matrix}}$ decreases less rapidly for the matrix containing additives than in the pure bulk case. Also note that, in contrast to the pure bulk, $\overline{f}_{\text{matrix}}$ does not go to zero at a finite temperature for the matrix containing additives with $k_p = k_p' = 0.40$. The additive sites do not disappear, and may continue to facilitate dormant sites to "wake up" (with probability $k_p' = 0.40$). Therefore, the additive sites provide a pathway for dormant sites in the surrounding matrix to become mobile via an additive facilitated "wake up" move that is not possible in the pure bulk.

2. Additive induced changes in T_g

Here we consider the effects of additives on the bulk glass transition temperature, T_g. Recall from the description of the LM model that T_g is defined as the temperature at which the steady state fraction of mobile sites $\overline{f}_{\text{matrix}} = 0.10$. Figure 4 shows what happens to the matrix T_g for the two scenarios in which the site fractions of inert additives, and additives parameterized to match the matrix, increase. The T_g values shown in Figure 4 have been normalized by the glass transition temperature of the pure bulk, which is given the symbol, $T_{g,0}$.

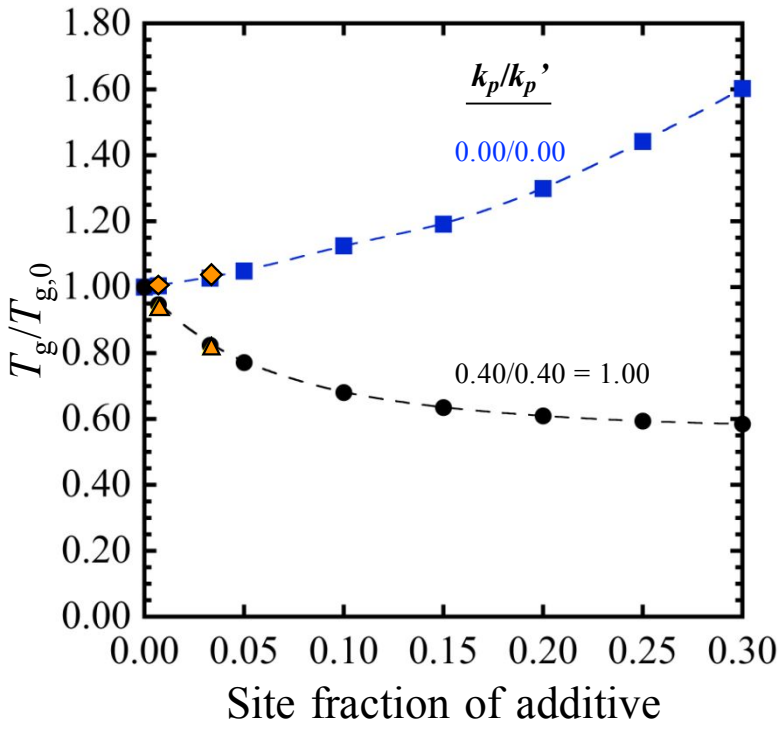

Figure 4: Plasticization and antiplasticization effects on T_g relative to the pure bulk value ($T_g/T_{g,0}$) as the site fraction of additives is increased. "Inert" additives ($k_p = k_p' = 0.00$) which enhance the matrix T_g are shown in blue, while plasticizing additives ($k = k' = k_p = k_p' = 0.40$) which reduce the matrix T_g are shown in black. Orange diamonds and triangles correspond to FA model simulation results[20] for a matrix system containing antiplasticizing and plasticizing nanoparticles, respectively.

Beginning with the inert additives (blue squares in Figure 4), we see that $T_g/T_{g,0}$ increases as their concentration increases; i.e., inert additive sites increase the matrix T_g relative to that of the pure bulk. These results suggest that inert additives in the LM model behave like an antiplasticizer, analogous to behavior that has been observed for systems such as polymer nanocomposites,[3,15,26,40,56] and PMMA/organic dyes[56], which are described further below.

Rittigstein et al.[22] measured the effect of silica nanoparticles on the bulk T_g values of PMMA, poly(2-vinylpyridine) (P2VP), and polystyrene (PS) via fluorescence measurements. Between 0 – 0.6 volume % of nanoparticles, the values of $T_g/T_{g,0}$ for these polymers ranged in value from approximately 1 – 1.01 for PMMA, 1 – 1.05 for P2VP, and no change was observed for PS. The authors suggested that attractive nanoparticle-polymer interactions (e.g., hydrogen bonding) may have slightly increased the strength of the T_g enhancement effect for PMMA and

P2VP relative to that of PS, although the effect is clearly very small. [22] Over this concentration range (i.e. less than 1%) of inert additive sites, our results indicate essentially no change in the value of $T_g/T_{g,0}$, which is consistent with experiment.

Mangalara and Simmons[3] performed MD simulations of flexible and stiff oligomeric additives in a bead-spring polymer melt. For 5.0 volume % of oligomeric additive, $T_g/T_{g,0}$ ranged in value from approximately 0.95 – 1.20 as the stiffness parameter, K, of the oligomer increased in value from 0 – 100. Using the LM model, $T_g/T_{g,0} = 1.05$ for a matrix system containing 5.0% inert additive sites, which is comparable to the value of $T_g/T_{g,0}$ reported by Mangalara and Simmons for a bead spring polymer melt containing 5.0 volume % of a relatively flexible ($K \approx 3.0$) oligomeric additive[3].

Our results (Figure 4) for the case of additive sites where $k_p = k_p' = 0.40$ (black circles), meaning the activity of such sites matches that of matrix sites, show that $T_g/T_{g,0}$ decreases as the site fraction of additives increases. This reduction in the matrix T_g is consistent with that reported for polymer/gas mixtures and other polymer/small molecule additive mixtures[3,11,15-20,28,34,38-40].

One such study was performed by Sanders, in which experimental measurements of $T_g/T_{g,0}$ for a set of six different polymers containing absorbed CO_2 were reported[31]. The $T_g/T_{g,0}$ values for the set of polymers lie roughly on a curve that varies from a value of 1 to approximately 0.55 as the concentration of absorbed CO_2 increases from 0 to 100 in units of cc(STP)/cc polymer. One polymer from this set is poly(ether sulfone) (PES), and Sanders reports that $T_g/T_{g,0} \approx 0.55$ for PES at 50 cc(STP)/cc polymer,[31] which corresponds to approximately 9 volume % CO_2[42]. For an LM matrix system containing 9% additive sites where $k_p = k_p' = 0.40$, we calculate that $T_g/T_{g,0} \approx 0.70$. While we find a slightly weaker plasticizing effect for additives with $k_p = k_p' = 0.40$ than the experimental results for PES/CO_2, note that the k_p and k_p' values have been fixed at the matrix parameter values, and not optimized to match any set of experimental data.

Finally, Fig. 4 also includes (orange diamonds and triangles) simulation results reported by Pryamitsyn and Ganesan[20] for the effect of a small (< 0.05) site fraction of additive using the Fredrickson-Anderson (FA) kinetically constrained Ising model. Pryamitsyn and Ganesan

simulated matrix systems containing anti/plasticizing particles which were incorporated as a collection of quenched "down" spins, while plasticizing particles were represented as a collection of quenched "up" spins. In their work they characterized the temperature dependence of the relaxation times for matrix systems containing anti/plasticizing particles using the FA model. These temperature dependent relaxation times were fit to the Vogel-Fulcher-Tammann (VFT) equation and a value for the VFT parameter, T_0, was determined. The value of the characteristic temperature parameter T_0 roughly tracks with the glass transition temperature T_g, thus Pryamitsyn and Ganesan approximated T_g values for their FA model simulations by using values of T_0[20]. Their $T_0/T_{0,\text{pure}}$ results for matrix systems containing anti/plasticizing particles, where the value of $T_{0,pure}$ is that for the pure bulk, are included in Figure 4. The plots show that the LM results are consistent with this earlier, limited, set using a different approach.

Overall, we find that the predicted range of $T_g/T_{g,0}$ values for bulk/additive systems using the LM model in two simple scenarios compares favorably with relevant experimental[25,26,31,32,47] and molecular dynamics (MD)[3,15,40] studies. We recognize that the number and chemical diversity of possible polymer/additive combinations is such that we cannot *explicitly* model all using our simple LM model approach. However, in the next section we illustrate how changing the values of k_p and k_p' allows for control over the strength of the additive induced effect on T_g.

3. How changing the additive-matrix interaction strength via k_p/k_p' affects T_g

Using the LM model, the values of the k_p and k_p' parameters can be changed such that the attempt probability of the additive facilitated "sleep" move is favored over that of the "wake up" move, or vice versa. In this way we can model the varying interaction strength between additive particles and the surrounding matrix. Figure 5 illustrates the extent to which additive sites can enhance or suppress the pure matrix T_g ($T_{g,0}$). The conditions cover a range of values individually for k_p and k_p', and for the ratio k_p/k_p' - which may or may not be kept constant as the individual values are changed.

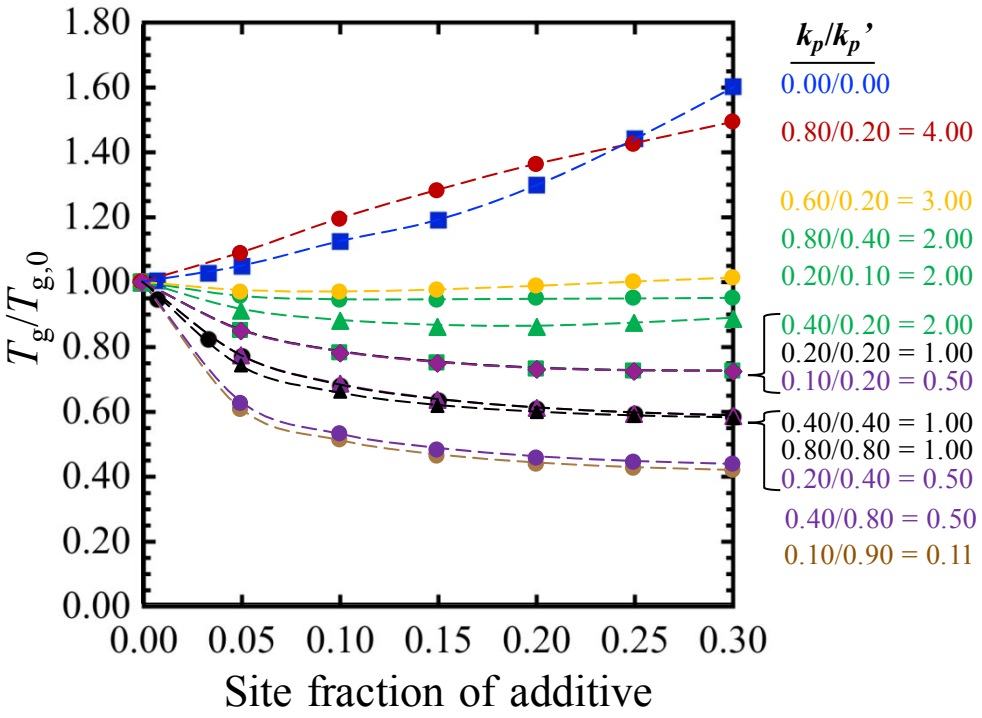

Figure 5: The effect of changing the additive "interaction strength" through varying the ratio k_p/k_p' on the matrix T_g. The $T_g/T_{g,0}$ values are plotted against the site fraction of additive, and the corresponding k_p/k_p' values for each set of results are shown to the right of the plot. Dashed lines are guides to the eye.

For the purpose of our discussion, it will be useful to divide the range of k_p/k_p' values shown in Figure 5 according to how T_g is affected; i.e., suppression, no change, and enhancement. Beginning with values of k_p/k_p' where $0.11 \leq k_p/k_p' \leq 2.00$, we find that additive sites reduce T_g relative to that of the pure bulk ($T_g/T_{g,0} < 1$). The strength of the T_g suppression effect is weakest for additives when $k_p/k_p' = 2.00$ (additive facilitated "sleep" move dominates over "wake up") and strongest for additives when $k_p/k_p' = 0.11$ (additive facilitated "wake up" move dominates over "sleep"). For each value of k_p/k_p' in this range, the extent of the matrix T_g suppression increases most strongly as the additive site content increases from 5%, and then more weakly as the additive fraction rises to 30%. Note that Figure 5 also indicates that in some cases, the effect on $T_g/T_{g,0}$ can be the *same* for *different* values of the ratio k_p/k_p'; e.g., $T_g/T_{g,0}$ trends corresponding to $k_p/k_p' = 0.40/0.20 = 2.00$ and $k_p/k_p' = 0.20/0.20 = 1.00$. We will return to this behavior in the next section.

Beginning with ratios k_p/k_p' greater than 2.00 we find that the effect of additive sites on $T_g/T_{g,0}$ changes from slight T_g suppression, to no change in T_g, to T_g enhancement. As shown in

Figure 5, the "null" effect roughly occurs when additive sites interact with the matrix such that $k_p/k_p' = 0.60/0.20$. For these additives, there is approximately no change in T_g relative to that of the pure bulk even when the system contains 30% additives.

Turning to additive induced T_g enhancement, we find that $k_p/k_p' > 3.00$ yield values of $T_g/T_{g,0} > 1$. For example, additive sites with $k_p/k_p' = 0.80/0.20 = 4.00$ yield values of $T_g/T_{g,0}$ between 1 and ~1.5 as the additive site fraction increases from 0 – 30%. Also note that the range of $T_g/T_{g,0}$ values for $k_p/k_p' = 0.80/0.20 = 4.00$ roughly matches that of a matrix containing inert additive sites ($k_p = k_p' = 0.00$). In the former case, because there is a modest value assigned to the attempt probability of the additive facilitated "wake up" move, k_p' (= 0.20), a relatively large value for the reverse "sleep" move, i.e., $k_p = 0.80$, dominates, yielding a comparable effect on T_g to the inert additive sites, that can never facilitate a neighbor's awakening.

4. How intrinsic matrix mobility is coupled with additive induced effects

In the previous section, we noted cases in which different ratios of k_p/k_p' yield the same resulting ratio of $T_g/T_{g,0}$. For example, with $k_p/k_p' = 0.40/0.20 = 2.00$ and $k_p/k_p' = 0.20/0.20 = 1.00$ the results for $T_g/T_{g,0}$ are approximately equal. This suggests that the individual values of k_p and k_p' for the additive sites can play a role in changing the matrix T_g, in addition to the dependence on the ratio k_p/k_p' covered in the previous section.

In Figure 6 we explore the linkage between matrix mobility (reflected in k, k') and additive influence (through k_p, k_p') in changing $T_g/T_{g,0}$, when the fraction of additive sites is fixed at 30%. In each scenario the effect is tracked as we increase the strength of the additive 'sleep' (k_p) move relative to the matrix 'wake up' move (k'), such that both $k = k'$ are fixed. Results are shown for three different kinds of additives, indicated by three ratios of $k_p/k_p' = 0.50$ (purple), 1.00 (black), and 2.00 (green).

Note that there are two sets of results shown: The filled point results correspond to fixed $k = k' = 0.40$ and the open point results correspond to fixed $k = k' = 0.25$. There is little difference between the two scenarios, both of which involve $k/k' = 1.0$, which implies that additive effects will be similar as long as the matrix material's 'wake up' and 'sleep' tendencies are balanced. Reading each plot from left to right can be interpreted as the effect of increasing the ability of the

additive (via k_p) to assist matrix sites in going dormant, with the matrix 'wake up' tendency (via k') fixed. Next, we draw some conclusions that apply to all three data sets.

In all cases the T_g for the matrix with additives increases rapidly as k_p approaches zero (k_p/k' -> 0 with k' fixed). Recall that "inert" additive sites ($k_p = k_p' = 0.00$) *enhance* the T_g of the matrix, because they reduce the probability that a dormant matrix site has a mobile neighbor to facilitate a matrix "wake up" move. Therefore, as the ratio k_p/k' goes to zero, the plasticizing effects of the additive facilitated "wake up" and "sleep" moves on the surrounding matrix are diminished, and the dominant influence of the additive sites on the matrix is shifted towards behaving like the "inert" additive sites (where additive sites reduce the probability that a dormant site has a mobile neighbor).

In the other direction, as k_p/k' increases the additives are becoming more effective at facilitating a mobile site to go dormant, relative to the matrix tendency to 'wake up' from a dormant state, given a mobile neighbor. We know from Figure 5 that, for a given concentration of additive, as this ratio decreases (with the matrix unchanging) then that additive becomes more effective at mobilizing the matrix material, and the glass transition temperature will become lower relative to bulk matrix. This trend is also shown in Figure 6, if we compare what happens to $T_g/T_{g,0}$ over the three data sets at a given, fixed, value of k_p/k'.

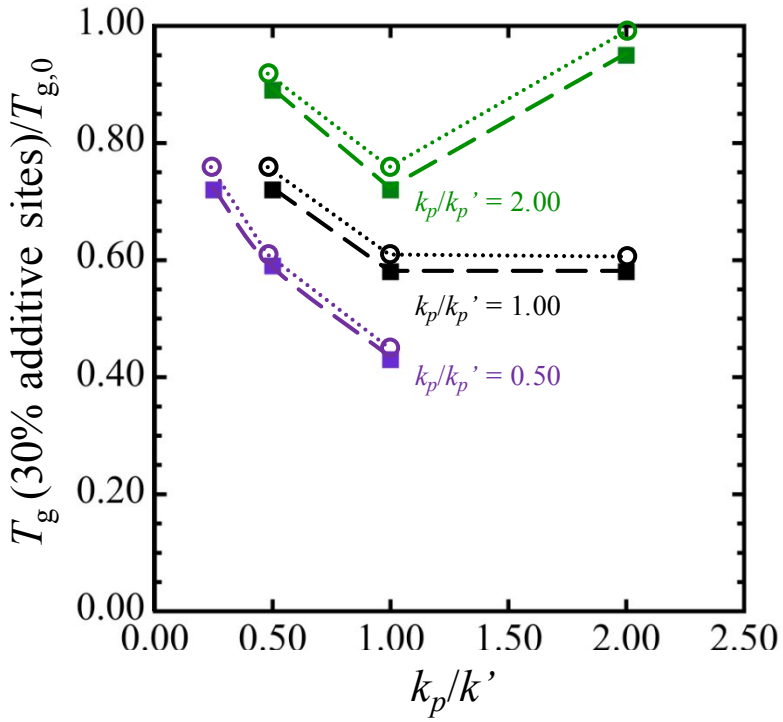

Figure 6: The effect of the individual values of the k_p and k_p' parameters on $T_g/T_{g,0}$ for matrix systems containing 30% additive sites. $T_g/T_{g,0}$ values are plotted for fixed ratios of $k_p/k_p' = 0.50$ (purple), 1.00 (black), and 2.00 (green) relative relative to the ratio k_p/k', which reflects the relative strength of the additive facilitated "sleep" move to that of the mobile site facilitated "wake up" move of the matrix. Filled points correspond to results for a matrix with $k = k' = 0.40$ and open points correspond to results for a matrix with $k = k' = 0.25$. Dashed lines serve as a guide to the eye.

Of the three sets of results in Figure 6 consider first those for additive sites with $k_p/k_p' = 0.50$ (bottom results, purple squares); in this case the probability of an additive 'sleep' effect is half that of the 'wake up'. In this series as k_p/k' increases (with k' fixed) the value of k_p' continues to be double that of k_p. In other words, the attempt probability of the additive facilitated "wake up" move is *always* twice as favorable as that of the additive facilitated "sleep" move, and the result is an increasing ability of the additive to suppress the material T_g value, relative to pure matrix. Indeed, the additives are so effective at suppressing T_g that for large enough k_p, (with k_p' double that value) the material remains a melt.

Turning to the results for a matrix containing additive sites with $k_p/k_p' = 1.00$ (shown in black), we find that the extent to which $T_g/T_{g,0}$ can be reduced by changing the individual values of k_p and k_p' is limited by the value of the matrix parameter k'. The value of $T_g/T_{g,0}$ decreases with increasing k_p/k' until that fraction becomes equal to 1.00, at which point the additive facilitated "wake up" and "sleep" moves are equivalently successful as the corresponding moves in the matrix material. Since for this data set the ratio of $k_p/k_p' = 1.00$ is fixed, the attempt probabilities of the forward and reverse additive facilitated moves are always equivalent. Therefore, any further increase in the individual values of k_p and k_p' beyond $k_p/k' = 1$ does not change $T_g/T_{g,0}$.

Finally, we examine the results corresponding to $k_p/k_p' = 2.00$ (shown in green) in Figure 6. Consistent with the other cases, we find that the value of $T_g/T_{g,0}$ decreases between $0 < k_p/k' \leq 1$. However, there is a noticeable difference in behavior such that as k_p/k' increases from 1.00 to 2.00, $T_g/T_{g,0}$ begins to increase. The matrix with these additives is becoming easier to turn glass i.e. the transition happens at higher temperatures, although still below the pure bulk glass transition. With $k_p/k_p' = 2.00$, as k_p increases the value of k_p' increases by only half as much; i.e., the attempt probability of the additive facilitated "sleep" is always more favorable than that of the

reverse "wake up" move. In this set of results, with $k_p/k' > 1$, then whether k' is fixed at 0.40 or 0.25, k_p will be larger than k_p', k, and k'. So the additive effect on dormancy dominates over both the matrix tendency to wake up and the additive ability to facilitate wake up. The net result is a significant rise in matrix tendency to go dormant, which raises the glass transition temperature relative to the case for all the other conditions.

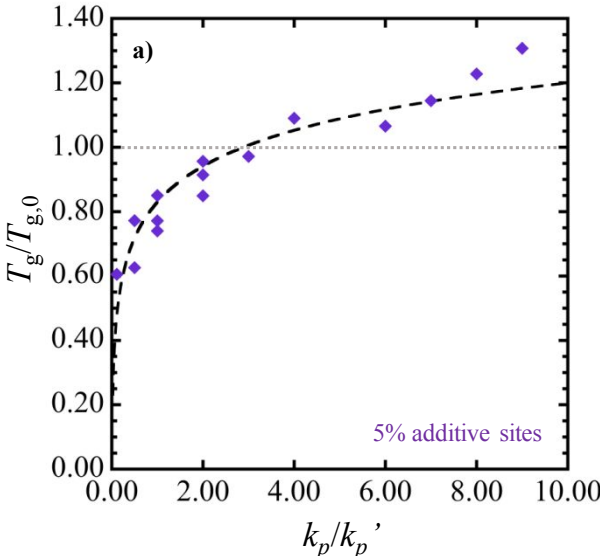

5. Broader T_g trends

In this section we show results for how $T_g/T_{g,0}$ changes as the ratio k_p/k_p' is increased over a much wider range than depicted so far, for three choices of additive site.

Figure 7 illustrates this for matrix systems containing (a)5.0%, (b)10%, and (c)30% additive sites. The range of k_p/k_p' spans from 0.11 to 9.00. In illustrating the results we combine those for different individual values of k_p and k_p' that yield the same ratio of k_p/k_p'; e.g., $k_p/k_p' = 0.40/0.40 = 1.00$ and $k_p/k_p' = 0.80/0.80 = 1.00$.

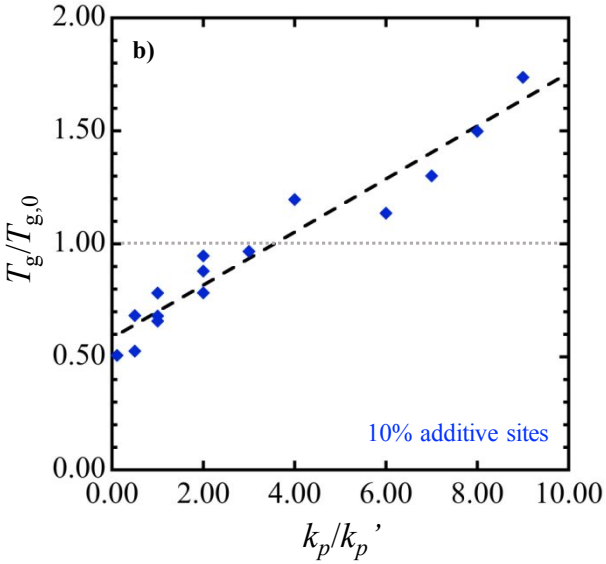

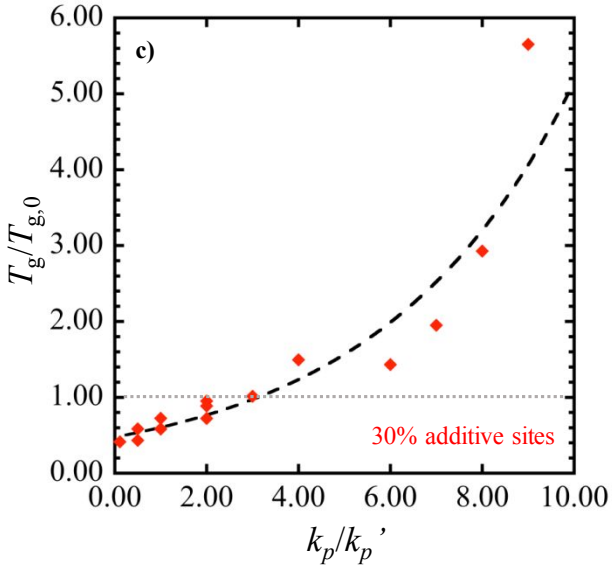

Figure 7: Trends in $T_g/T_{g,0}$ with respect to the ratio k_p/k_p' for matrix systems containing 5% **(a)**, 10% **(b)**, and 30% **(c)** additive sites. Dashed lines are best fit functions to the results, which correspond to: logarithmic **(a)**, linear **(b)**, and exponential **(c)** fits. Light grey dotted lines indicate $T_g = T_{g,0}$.

In all three parts of Figure 7 we see $T_g/T_{g,0}$ increases as the ratio k_p/k_p' varies from 0.11 to 9.00; the material turns glassy at higher temperatures as the additive facilitated "sleep" move becomes more important relative to the "wake up" move. This trend becomes more pronounced as the amount of additive is increased. For a matrix system containing 5.0% additive sites (Figure 7a), $T_g/T_{g,0}$ ranges in value from approximately 0.50 to 1.35 over the range of k_p/k_p'; as the dashed best-fit line shows, in this case $T_g/T_{g,0}$ roughly goes as $\ln(k_p/k_p')$. This LM trend matches well with comparable results obtained via molecular dynamics simulations reported by Simmons and coworkers[3]. In their work, $T_g/T_{g,0}$ was determined for a polymer matrix containing 5 vol. % oligomeric additives, in which the stiffness parameter of the bending potential, K, for the oligomers was varied. As the value of K was increased from 0 (flexible) to 100 (nearly rod-like), $T_g/T_{g,0}$ increased from 0.93 to 1.25,[3] which compares modestly well with the range of $T_g/T_{g,0} = 0.50$ to 1.35 that we find by varying k_p/k_p' between 0.11 to 9.00 using the LM model. Our results suggest a connection between additive molecule stiffness and the degree to which additive sites shift the matrix T_g as reflected in the success of assisting a neighbor to "sleep" relative to that of "waking up".

Turning to a matrix system containing 10% additive sites (Figure 7b), we find that the change in $T_g/T_{g,0}$ is roughly linear as k_p/k_p' increases such that, over the range of k_p/k_p' = 0.11 to 9.00, the value of $T_g/T_{g,0}$ increases from approximately 0.50 to 1.73. Finally, increasing the additive site fraction to 30% has the greatest effect on the matrix T_g (Figure 7c). In this case, we find that $T_g/T_{g,0}$ increases roughly exponentially with k_p/k_p' (i.e., $T_g/T_{g,0} \sim \exp[k_p/k_p']$), and varies in value from approximately 0.50 to 5.65 between k_p/k_p' = 0.11 and 9.00.

In general, these results confirm the expectation that small changes in additive character (as reflected in changes in the ratio k_p/k_p') will have a more dramatic effect on matrix T_g as the amount of additive is increased; indeed, the implication is that appreciable concentrations of the additive sites may glassify the matrix at a temperature well above the pure bulk T_g.

Summary and Conclusions

In this work we use the Limited Mobility (LM) model to simulate bulk/additive mixtures for the first time. By controlling additive properties and their interaction strength with the surrounding matrix we are able to show their potential for altering the mobility and glass transition temperature, T_g, of the matrix. Our results provide insight for a broad array of systems in which small molecule additives influence the properties of their surrounding matrix, including: membranes for gas separation[8-11,19,25-34] and polymer nanocomposites[15-22]. Because these materials are generally utilized in their glassy state, any potential influence of an additive on T_g is an important engineering consideration.

Matrix sites in the LM model have three possible states: “mobile”, “dormant”, and “dense”; a site can change its nature with a probability that is both matrix and temperature dependent. As opposed to sites containing matrix material, additive sites remain constant in their nature, regardless of temperature. However, they can influence local mobility by facilitating a neighboring mobile matrix site to become dormant (with probability k_p) or facilitating a neighboring dormant site to become mobile (with probability k_p’). We find that the ratio k_p/k_p’ can control the extent to which the mobility of the matrix is enhanced or diminished, and yields varying degrees of T_g suppression or enhancement relative to that of a pure bulk fluid ($T_{g,0}$). The results obtained using the LM model map well to experimental measurements of the effect of carbon

dioxide sorption on T_g for a number of different polymer species,[25,30,31,47] other kinetic lattice model simulations of a matrix containing anti/plasticizing particles approaching T_g,[20] and molecular dynamics (MD) simulations of oligomeric molecules added to a polymer melt approaching T_g[3,15,40].

The effects of additives can be controlled in a number of ways. The nature of the additives is set through the ratio of k_p/k_p' , which can be 'tuned' to cause T_g suppression or T_g enhancement of the matrix. For any fixed value of k_p/k_p', an increase in the site fraction of additive sites strengthens the effect of the additives on the local mobility, and thus T_g. Our comparisons with experimental[31] and simulation[3,20] results for the effects of additives on T_g suggest a possible connection between the ratio k_p/k_p' with the molecular properties of real additives; e.g., stiffness. Further, changing the individual values of k_p and k_p' for a fixed ratio of k_p/k_p' can also lead to a change in the magnitude of the additive sites effect on T_g. In this scenario, the relative influence of the additive sites on the matrix mobility is changing in comparison to the intrinsic mobility of the matrix itself.

The matrix mobility is determined by the k and k' parameters, which represent the mobile to dormant and facilitated dormant to mobile transitions of the matrix. More than just the independent nature of the additive, the properties of additive *relative to matrix* are key. When $k_p/k' < 1$, the local influence of additive sites on the matrix mobility is weak compared to the matrix itself. On the other hand, the effect of the additive sites on matrix mobility is dominant when $k_p/k' > 1$. Therefore, the individual values of k_p and k_p', which characterize the strength of the influence of additive sites on the local mobility of the matrix, must also be evaluated relative to the intrinsic mobility of the matrix itself.

We also find that the strength of the dependence of T_g on the ratio k_p/k_p' changes with additive site concentration. For a matrix system containing 5% additive sites, $T_g/T_{g,0}$ increases approximately logarithmically with respect to k_p/k_p', which semi-quantitatively matches results reported for MD simulations of polymer melt/5 vol. % oligomeric additive mixtures in which the stiffness parameter of the oligomeric molecules was varied[3]. By increasing the additive site fraction to 10%, the LM model predicts a roughly linear dependence of $T_g/T_{g,0}$ on k_p/k_p', while a further increase to 30% additive sites yields an approximately exponential dependence of $T_g/T_{g,}0$

on k_p/k_p'. These results provide predictive insight for the range of possible T_g effects that may occur upon changing the additive concentration and/or the influence of the additives on matrix mobility in a bulk/additive mixture.

In future work, it will be possible to extend this approach to additive-containing film samples, where a number of properties can be probed, one example being how additive sites affect the thickness-dependent T_g behavior of films. Some studies have shown that selecting an additive molecule of a particular chemical nature can effectively negate the influence of a free surface such that a bulk T_g value is observed in nanometrically thin films[1,2,21,22,38]. Another application of this LM model approach will be to simulate the transport of additive sites through a membrane, which would provide insight about the role of local mobilty in influencing diffusion through a glassy membrane.

AUTHOR INFORMATION

Corresponding Author

*E-mail: jane.lipson@dartmouth.edu

ORCID

Jane E. G. Lipson: 0000-0002-0177-9373

Notes

There are no conflicts to declare.

Acknowledgments

The authors gratefully acknowledge financial support from the National Science Foundation (DMR-1403757 and DMR-1708542) to J.E.G.L and Graduate Assistance in Areas of National

Need (GAANN) to JD. J.E.G.L. also acknowledges the Radcliffe Institute for Advanced Study at Harvard University.

References

[1] Ellison, C. J.; Ruszkowski, R. L.; Fredin, N. J.; Torkelson, J. M. Dramatic reduction of the effect of nanoconfinement on the glass transition of polymer films via addition of small-molecule diluent. *Phys. Rev. Lett.* 2004*,* **92**, 095702-095702.

[2] Ellison, C.; Kim, S.; Hall, D.; Torkelson, J. Confinement and processing effects on glass transition temperature and physical aging in ultrathin polymer films: Novel fluorescence measurements. *European Physical Journal E* 2002*,* **8**, 155-166.

[3] Mangalara, J. H.; Simmons, D. S. Tuning Polymer Glass Formation Behavior and Mechanical Properties with Oligomeric Diluents of Varying Stiffness. *Acs Macro Letters* 2015*, 4*, 1134-1138.

[4] Bondar, V. I.; Freeman, B. D.; Pinnau, I. Gas sorption and characterization of poly(ether-b-amide) segmented block copolymers. *Journal of Polymer Science Part B-Polymer Physics* 1999*,* **37**, 2463-2475.

[5] Chiou, J. S.; Maeda, Y.; Paul, D. R. Gas and Vapor Sorption in Polymers just Below Tg. *J Appl Polym Sci* 1985, **30**, 4019-4029.

[6] De Angelis, M. G.; Sarti, G. C. Solubility of Gases and Liquids in Glassy Polymers. *Annual Review of Chemical and Biomolecular Engineering, Vol 2* 2011, **2**, 97-120.

[7] Domack, A.; Johannsmann, D. Plastification during sorption of polymeric thin films: A quartz resonator study. *J. Appl. Phys.* 1996, **80**, 2599-2604.

[8] Hoelck, O.; Boehning, M.; Heuchel, M.; Siegert, M. R.; Hofmann, D. Gas sorption isotherms in swelling glassy polymers-Detailed atomistic simulations. *J. Membr. Sci.* 2013, **428**, 523-532.

[9] Koros, W. J.; Paul, D. R. Co2 Sorption in Poly(ethylene-Terephthalate) Above and Below Glass-Transition. *Journal of Polymer Science Part B-Polymer Physics* 1978, **16**, 1947-1963.

[10] Koros, W. J.; Paul, D. R.; Rocha, A. A. Carbon-Dioxide Sorption and Transport in Polycarbonate. *Journal of Polymer Science Part B-Polymer Physics* 1976, **14,** 687-702.

[11] Meunier, M. Diffusion coefficients of small gas molecules in amorphous cis-1,4-polybutadiene estimated by molecular dynamics simulations. *J. Chem. Phys.* 2005, **123**, 134906-134906.

[12] Mukherjee, M.; Chebil, M. S.; Delorme, N.; Gibaud, A. Power law in swelling of ultra-thin polymer films. *Polymer* 2013, **54,** 4669-4674.

[13] Ogieglo, W.; Wormeester, H.; Eichhorn, K.; Wessling, M.; Benes, N. E. In situ ellipsometry studies on swelling of thin polymer films: A review. *Progress in Polymer Science* 2015, **42,** 42-78.

[14] Miwa, Y.; Kondo, T.; Kutsumizu, S. Subnanoscopic Mapping of Glass Transition Temperature around Ionic Multiplets in Sodium-Neutralized Poly(ethylene-random-methacrylic acid) Ionomer. *Macromolecules* 2013, **46**, 5232-5237.

[15] Betancourt, B. A. P.; Douglas, J. F.; Starr, F. W. Fragility and cooperative motion in a glass-forming polymer-nanoparticle composite. *Soft Matter* 2013, **9**, 241-254.

[16] Starr, F. W.; Schroder, T. B.; Glotzer, S. C. Molecular dynamics simulation of a polymer melt with a nanoscopic particle. *Macromolecules* 2002, **35**, 4481-4492.

[17] Starr, F. W.; Schroder, T. B.; Glotzer, S. C. Effects of a nanoscopic filler on the structure and dynamics of a simulated polymer melt and the relationship to ultrathin films. *Physical Review E* 2001, **64**, 021802-021802.

[18] Starr, F. W.; Douglas, J. F. Modifying Fragility and Collective Motion in Polymer Melts with Nanoparticles. *Phys. Rev. Lett.* 2011, **106**, 115702-115702.

[19] Hanson, B.; Pryamitsyn, V.; Ganesan, V. Computer Simulations of Gas Diffusion in Polystyrene-C-60 Fullerene Nanocomposites Using Trajectory Extending Kinetic Monte Carlo Method. *J Phys Chem B* 2012, **116**, 95-103.

[20] Pryamitsyn, V.; Ganesan, V. A Comparison of the Dynamical Relaxations in a Model for Glass Transition in Polymer Nanocomposites and Polymer Thin Films. *Macromolecules* 2010, **43**, 5851-5862.

[21] Bansal, A.; Yang, H. C.; Li, C. Z.; Cho, K. W.; Benicewicz, B. C.; Kumar, S. K.; Schadler, L. S. Quantitative equivalence between polymer nanocomposites and thin polymer films. *Nature Materials* 2005, **4**, 693-698.

[22] Rittigstein, P.; Priestley, R. D.; Broadbelt, L. J.; Torkelson, J. M. Model polymer nanocomposites provide an understanding of confinement effects in real nanocomposites. *Nature Materials* 2007, **6**, 278-282.

[23] Kumar, S. K., Ganesan, V. ; Riggleman, R. A. Perspective: Outstanding theoretical questions in polymer-nanoparticle hybrids. *J. Chem. Phys.* , 2017, **147**, 020901.

[24] Baeza, G. P., Dessi, C., Costanzo, S., Zhao, D., Gong, S., Alegria, A., Colby, R. H., Rubinstein, M., Vlassopoulos, D. & Kumar, S. K. Network dynamics in nanofilled polymers. *Nat. Commun.* 2016, **7**, 11368.

[25] Gutierrez, C.; Francisco Rodriguez, J.; Gracia, I.; de Lucas, A.; Teresa Garcia, M. Modification of polystyrene properties by CO2: Experimental study and correlation. *J Appl Polym Sci* 2015, **132**, 41696-41696.

[26] Psurek, T.; Soles, C. L.; Page, K. A.; Cicerone, M. T.; Douglas, J. F. Quantifying Changes in the High-Frequency Dynamics of Mixtures by Dielectric Spectroscopy. *J Phys Chem B* 2008, **112**, 15980-15990.

[27] Stanciu, N. V., Stan, F. & Fetecau, C. Melt Shear Rheology and pVT Behavior of Polypropylene/Multi-Walled Carbon Nanotube Composites. *Mater. Plast,*2018, **55**, 482–487.

[28] Sanders, D. E.; Smith, Z. P.; Guo, R.; Robeson, L. M.; McGrath, J. E.; Paul, D. R.; Freeman, B. D. Energy Efficient Polymeric Gas Separation Membranes for a Sustainable Future: A Review. *Polymer* 2013, **54**, 4729–4761.

[29] Baker, R. W.; Low, B. T. Gas Separation Membrane Materials: A Perspective. *Macromolecules* 2014, 47, 6999–7013.

[30] Bos, A.; Punt, I. G. M.; Wessling, M.; Strathmann, H. CO2-induced plasticization phenomena in glassy polymers. *J. Membr. Sci.* 1999, **155**, 67-78.

[31] Sanders, E. S. Penetrant-Induced Plasticization and Gas Permeation in Glassy-Polymers. *J. Membr. Sci.* 1988, **37,** 63-80.

[32] Minelli, M.; Sarti, G. C. Permeability and diffusivity of CO2 in glassy polymers with and without plasticization. *J. Membr. Sci.* 2013, **435**, 176-185.

[33] Neyertz, S.; Brown, D.; Pandiyan, S.; van der Vegt, N. F. A. Carbon Dioxide Diffusion and Plasticization in Fluorinated Polyimides. *Macromolecules* 2010, **43**, 7813-7827.

[34] Saxton, J. M. Lateral Diffusion in an Archipelago - the Effect of Mobile Obstacles. *Biophys. J.* 1987, **52**, 989–997.

[35] Yong, W. F.; Kwek, K. H. A.; Liao, K.; Chung, T. Suppression of aging and plasticization in highly permeable polymers. *Polymer* 2015, **77**, 377-386.

[36] Lau, C. H.; Li, P.; Li, F.; Chung, T.; Paul, D. R. Reverse-Selective Polymeric Membranes for Gas Separations. *Progress in Polymer Science* 2013, **38**, 740–766.

[37] Ismail, A. F.; Lorna, W. Penetrant-induced plasticization phenomenon in glassy polymers for gas separation membrane. *Separation and Purification Technology* 2002, **27**, 173–194.

[38] Evans, C. M.; Deng, H.; Jager, W. F.; Torkelson, J. M. Fragility is a Key Parameter in Determining the Magnitude of T-g-Confinement Effects in Polymer Films. *Macromolecules* 2013, **46**, 6091-6103.

[39] Pandiyan, S.; Brown, D.; Neyertz, S.; van der Vegt, N. F. A. Carbon Dioxide Solubility in Three Fluorinated Polyimides Studied by Molecular Dynamics Simulations. *Macromolecules* 2010, **43**, 2605-2621.

[40] Stukalin, E. B.; Douglas, J. F.; Freed, K. F. Plasticization and antiplasticization of polymer melts diluted by low molar mass species. *J. Chem. Phys.* 2010, **132**, 084504-084504.

[41] Tito, N. B.; Lipson, J. E. G.; Milner, S. T. Lattice model of mobility at interfaces: free surfaces, substrates, and bilayers. *Soft Matter* 2013, **9**, 9403-9413.

[42] Tito, N. B.; Lipson, J. E. G.; Milner, S. T. Lattice model of dynamic heterogeneity and kinetic arrest in glass-forming liquids. *Soft Matter* 2013, **9**, 3173-3180.

[43] DeFelice, J.; Milner, S. T.; Lipson, J. E. G. Simulating Local T-g Reporting Layers in Glassy Thin Films. *Macromolecules* 2016*,* **49**, 1822-1833.

[44] Tito, N. B.; Milner, S. T.; Lipson, J. E. G. Enhanced diffusion and mobile fronts in a simple lattice model of glass-forming liquids. *Soft Matter* 2015*,* **11**, 7792-7801.

[45] DeFelice, J.; Lipson, J. E. G. Different metrics for connecting mobility and glassiness in thin films. *Soft Matter* 2019, **15**, 1651- 1657.

[46] Chiou, J. S.; Barlow, J. W.; Paul, D. R. Plasticization of Glassy-Polymers by Co2. *J Appl Polym Sci* 1985*,* **30**, 2633-2642.

[47] Kasturirangan, A.; Koh, C. A.; Teja, A. S. Glass-Transition Temperatures in CO2 + Polymer Systems: Modeling and Experiment. *Ind Eng Chem Res* 2011*,* **50**, 158-162.

[48] Ogieglo, W.; Wessling, M.; Benes, N. E. Polymer Relaxations in Thin Films in the Vicinity of a Penetrant- or Temperature-Induced Glass Transition. *Macromolecules* 2014*,* **47**, 3654-3660.

[49] Ribeiro, C. P.,Jr.; Freeman, B. D. Sorption, Dilation, and Partial Molar Volumes of Carbon Dioxide and Ethane in Cross-Linked Poly(ethylene oxide). *Macromolecules* 2008*,* **41**, 9458-9468.

[50] Carroll, B., Cheng, S. & Sokolov, A. P. Analyzing the Interfacial Layer Properties in Polymer Nanocomposites by Broadband Dielectric Spectroscopy. *Macromolecules* 50, 2017, 6149–6163.

[51] Heuchel, M.; Boehning, M.; Holck, O.; Siegert, M. R.; Hofmann, D. Atomistic packing models for experimentally investigated swelling states induced by CO2 in glassy polysulfone and poly(ether sulfone). *Journal of Polymer Science Part B-Polymer Physics* 2006*,* **44**, 1874-1897.

[52] Betancourt, B. A. P.; Hanakata, P. Z.; Starr, F. W.; Douglas, J. F. Quantitative relations between cooperative motion, emergent elasticity, and free volume in model glass-forming polymer materials. *Proc. Natl. Acad. Sci. U. S. A.* 2015*,* **112**, 2966-2971.

[53] Emamy, H., Kumar, S. K. & Starr, F. W. Diminishing Interfacial Effects with Decreasing Nanoparticle Size in Polymer-Nanoparticle Composites. *Phys. Rev. Lett.* 121, 2018, 207801.

[54] Jordan, W. J.; Koros, S. S. A free-volume distribution model of gas sorption and dilation in glassy-polymers. *Macromolecules* 1995, **28**, 2228–2235.

[55] Dorenbos, G.; Morohoshi, K. Modeling gas permeation through membranes by kinetic monte carlo: Applications to H2, O2, and N2 in hydrated Nafion ®. *J. Chem. Phys.* 2011, **134**, 044133.

[56] Kalogeras, I. M.; Pallikari, F.; Vassilikou-Dova, A. The diverse effect of antiplasticizer in the molecular dynamics of an organic dye-doped polymer observed at different motional lengthscales. *European Polymer Journal* 2009*,* **45**, 1377-1384.

[57] Ediger, M. D.; Forrest, J. A. Dynamics near Free Surfaces and the Glass Transition in Thin Polymer Films: A View to the Future. *Macromolecules* 2014*,* **47**, 471-478.

[58] Qi, D.; Fakhraai, Z.; Forrest, J. A. Substrate and chain size dependence of near surface dynamics of glassy polymers. *Phys. Rev. Lett.* 2008, **101**, 096101.

[59] Qi, D.; Ilton, M.; Forrest, J. A. Measuring surface and bulk relaxation in glassy polymers. *European Physical Journal E* 2011, **34**, 56.

[60] Mirigian, S.; Schweizer, K. S. Communication: Slow relaxation, spatial mobility gradients, and vitrification in confined films. *J. Chem. Phys.* 2014, **141**, 161103.

[61] Ye, C.; Wiener, C. G.; Tyagi, M.; Uhrig, D.; Orski, S. V.; Soles, C. L.; Vogt, B. D.; Simmons, D. S.. Understanding the decreased segmental dynamics of supported thin polymer films reported by incoherent neutron scattering. *Macromolecules* 2015, **48**, 801–808.

[62] Xia, W.; Mishra, S.; Keten, S. Substrate vs. free surface: Competing effects on the glass transition of polymer thin films. *Polymer* 2013, **54**, 5942–5951.

[63] Kim, S.; Torkelson, J. M. Distribution of Glass Transition Temperatures in Free-Standing, Nanoconfined Polystyrene Films: A Test of de Gennes' Sliding Motion Mechanism. *Macromolecules* 2011*,* **44**, 4546-4553.

[64] Roth, C. B.; Torkelson, J. M. Selectively probing the glass transition temperature in multilayer polymer films: Equivalence of block copolymers and multilayer films of different homopolymers. *Macromolecules* 2007*,* **40**, 3328-3336.

[65] Baglay, R. R.; Roth, C. B. Communication: Experimentally determined profile of local glass transition temperature across a glassy-rubbery polymer interface with a T-g difference of 80 K. *J. Chem. Phys.* 2015*,* **143**, 111101-111101.

[66] Lang, R. J.; Merling, W. L.; Simmons, D. S. Combined dependence of nanoconfined Tg on interfacial energy and softness of confinement. *ACS Macro Letters* 2014, **3**, 758–762.

[67] Keddie, J. L.; Jones, R. A. L.; Cory, R. A. Size-Dependent Depression of the Glass-Transition Temperature in Polymer-Films. *Europhys. Lett.* 1994*,* **27**, 59-64.

[68] Fryer, D. S.; Nealey, P. F.; de Pablo, J. J. Thermal probe measurements of the glass transition temperature for ultrathin polymer films as a function of thickness. *Macromolecules* 2000, **33**, 6439–6447.

[69] Salez, T.; Salez, J.; Dalnoki-Veress, K.; Raphael, E.; Forrest, J. A. Cooperative strings and glassy interfaces. *Proc. Natl. Acad. Sci.* 2015, **112**, 8227–8231.

[70] Cheng, S., Carroll, B., Lu, W., Fan, F., Carrillo, J.-M. Y., Martin, H., Holt, A. P., Kang, N.-G., Bocharova, V., Mays, J. W., Sumpter, B. G., Dadmun, M. & Sokolov, A. P. Interfacial Properties of Polymer Nanocomposites: Role of Chain Rigidity and Dynamic Heterogeneity Length Scale. *Macromolecules* 50, 2017, 2397–2406.

[71] Cheng, S., Carroll, B., Bocharova, V., Carrillo, J.-M. Y., Sumpter, B. G. & Sokolov, A. P. Focus: Structure and dynamics of the interfacial layer in polymer nanocomposites with attractive interactions. *J. Chem. Phys.* 146, 2017, 203201.

[72] Mattsson, J.; Forrest, J. A.; Borjesson, L. Quantifying glass transition behavior in ultrathin free-standing polymer films. *Physical Review E* 2000*,* **62**, 5187-5200.

[73] Ellison, C. J.; Torkelson, J. M. The distribution of glass-transition temperatures in nanoscopically confined glass formers. *Nature Materials* 2003*,* **2**, 695-700.

[74] Paeng, K.; Ediger, M. D. Molecular motion in free-standing thin films of poly(methyl methacrylate), poly(4-tert-butylstyrene), poly(alpha-methylstyrene), and poly(2-vinylpyridine). *Macromolecules* 2011, **44**, 7034–7042.

[75] Paeng, K.; Swallen, S. F.; Ediger, M. D. Direct measurement of molecular motion in freestanding polystyrene thin films. *J. Am. Chem. Soc.* 2011, **133**, 8444– 8447.

[76] Paeng, K.; Richert, R.; Ediger, M. D. Molecular mobility in supported thin films of polystyrene, poly(methyl methacrylate), and poly(2-vinyl pyridine) probed by dye reorientation. *Soft Matter* 2012, **8**, 819–826.

[77] Baeumchen, O.; McGraw, J. D.; Forrest, J. A.; Dalnoki-Veress, K. Reduced Glass Transition Temperatures in Thin Polymer Films: Surface Effect or Artifact? *Phys. Rev. Lett.* 2012*,* **109**, 055701-055701.

[78] Fakhraai, Z.; Forrest, J. A. Measuring the surface dynamics of glassy polymers. *Science* 2008, **319**, 600–604.

[79] Zuo, B.; Liu, Y.; Wang, L.; Zhu, Y.; Wang, Y.; Wang, X. Depth profile of the segmental dynamics at a poly(methyl methacrylate) film surface. *Soft Matter* 2013, **9**, 9376–9384.

[80] Meyers, G. F.; Dekoven, B. M.; Seitz, J. T. Is the molecular surface of polystyrene really glassy. *Langmuir* 1992, **8**, 2330–2335.

[81] Rauscher, P. M.; Pye, J. E.; Baglay, R. R.; Roth, C. B. Effect of Adjacent Rubbery Layers on the Physical Aging of Glassy Polymers. *Macromolecules* 2013*, 46*, 9806-9817.

[82] Frenken, J. W. M.; Vanderveen, J. F. Observation of surface melting. *Phys. Rev. Lett.* 1985, **54**, 134–137.

[83] Yang, Z.; Fujii, Y.; Lee, F. K.; Lam, C.; Tsui, O. K. C. Glass transition dynamics and surface layer mobility in unentangled polystyrene films. *Science* 2010, **328**, 1676–1679.

[84] Lan, T.; Torkelson, J. M. Methacrylate-based polymer films useful in lithographic applications exhibit different glass transition temperature-confinement effects at high and low molecular weight. *Polymer* 2014*,* **55**, 1249-1258.

[85] Roth, C. B.; McNerny, K. L.; Jager, W. F.; Torkelson, J. M. Eliminating the enhanced mobility at the free surface of polystyrene: Fluorescence studies of the glass transition temperature in thin bilayer films of immiscible polymers. *Macromolecules* 2007*,* **40**, 2568-2574.

[86] Baschnagel, J.; Varnik, F. Computer simulations of supercooled polymer melts in the bulk and in confined geometry. *Journal of Physics Condensed Matter* 2005, **17**, R851–R953.

[87] Jain, T. S.; de Pablo, J. J. Investigation of transition states in bulk and freestanding film polymer glasses. *Phys. Rev. Lett.* 2004, **92**, 155505.

[88] Shavit, A.; Riggleman, R. A. Influence of backbone rigidity on nanoscale confinement effects in model glass forming polymers. *Macromolecules* 2013, **46**, 5044–5052.

[89] Delaye, J. M.; Limoge, Y. Simulation of vacancies in a Lennard-Jones glass. *J. Non Cryst. Solids* 1993, **156**, 982–985.

[90] Donati, C.; Glotzer, S. C.; Poole, P. H.; Kob, W.; Plimpton, S. J. Spatial correlations of mobility and immobility in a glass forming Lennard-Jones liquid. *Physical Review E* 1999, **60**, 3107–3119.

[91] Fredrickson, G. H.; Andersen, H. C. Facilitated Kinetic Ising-Models and the Glass-Transition. *J. Chem. Phys.* 1985*,* **83**, 5822-5831.

[92] Lipson, J. E. G.; Milner, S. T. Percolation model of interfacial effects in polymeric glasses. *European Physical Journal B* 2009, **72**, 133–137.

For Table of Contents use only

The Influence of Additives on Polymer Matrix Mobility and T_g

Jeffrey DeFelice, Jane E. G. Lipson